International Journal of Thermophysics, Vol. 9, No. 3, 1988

Measurement of the Surface Tensions and the Interfacial Tensions of *n*-Pentane–Water and R 113–Water Systems

H. Matsubara,[1,2] M. Murase,[1,3] Y. H. Mori,[1] and A. Nagashima[1]

Received March 4, 1988

The surface and the interfacial tensions of mutually immiscible liquid systems were experimentally studied. The measured systems are *n*-pentane–water and R 113–water, which are proposed as heat transfer fluids for a direct-contact heat exchanger to be used for geothermal and waste heat recovery plants. The experimental apparatus was constructed based on the principle of the pendant drop method. Measurements were performed in the temperature range from 20 to 150°C. Based on the correlation of the surface and the interfacial tensions, the temperature dependences of the spreading coefficient, the film pressure, and the work of adhesion in each system were calculated.

KEY WORDS: adhesion; interfacial tension; *n*-pentane; pendant drop method; R 113; spreading coefficient; surface tension; water.

1. INTRODUCTION

The study of heat transfer between two immiscible liquids is important in the development of direct-contact heat exchangers considering potential application to geothermal and waste heat recovery plants. Direct-contact heat transfer between two immiscible liquids is affected by the behavior of the interfacial tension between these liquids and of the surface tension of each liquid contacting with the vapors of both liquids [1, 2]. In spite of the necessity of information on surface and interfacial tensions of these heat transfer fluids, only a limited amount of data is available. In the present

[1] Department of Mechanical Engineering, Keio University, Yokohama 223, Japan.
[2] Present address: Ishikawajima-Harima Heavy Industries Co., Ltd. 9-7, 2-Chome, Yaesu, Chuo-ku, Tokyo 104, Japan.
[3] Present address: Bridgestone Co., Ltd. 1-Chome, Kashiwao-machi, Totsuka-ku, Yokohama-shi, Kanagawa 224, Japan.

0195-928X/88/0500-0409$06.00/0

study, the surface tensions and the interfacial tensions were measured by the pendant drop method in the temperature range from room temperature up to 150°C. An apparatus for measurements up to 5 MPa in pressure has recently been constructed for this study. Having confirmed the reliability of this apparatus by measuring the surface tension of water at temperatures up to 200°C, the surface and the interfacial tensions of *n*-pentane–water and R 113–water systems were measured. These systems are proposed as heat transfer liquids for direct-contact heat exchangers. Based on correlations of the surface and the interfacial tensions, the temperature dependences of the spreading coefficient, the film pressure, and the work of adhesion in each system were calculated.

2. PRINCIPLE

The pendant drop method for determining the surface and the interfacial tensions can eliminate the effect of contacting solid surface. As shown in Fig. 1, the pendant drop of the sample liquid is formed at the tip of the

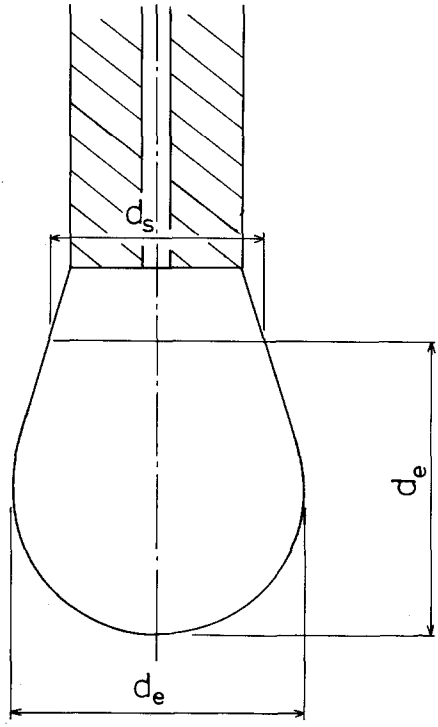

Fig. 1. Pendant drop.

capillary tube, which is vertically set in the cell; and by measuring the profile of the drop, the surface and the interfacial tensions are calculated. The equatorial diameter d_e and the diameter d_s of the drop in a selected plane which is located a distance d_e from the apex of the pendant drop are measured, and by the following equations, the surface and the interfacial tensions are calculated:

$$\sigma = \frac{\Delta\rho\, g d_e^2}{H} \tag{1}$$

$$1/H = f(s) = f(d_s/d_e) \tag{2}$$

where σ is the surface or the interfacial tension, $\Delta\rho$ is the density difference across the interface, and g is the acceleration due to gravity. The quantity $1/H$ is a function of $s = d_s/d_e$, which is given by Misak [3] as the following:

$$\begin{aligned}
&\text{for } s = 0.401 \text{ to } 0.46,\\
&1/H = (0.32720/s^{2.56651}) - 0.97553\, s^2 + 0.84059\, s - 0.18069\\
&\text{for } s \geqslant 0.46 \text{ to } 0.59,\\
&1/H = (0.31968/s^{2.59725}) - 0.46898\, s^2 + 0.50059\, s - 0.13261\\
&\text{for } s \geqslant 0.59 \text{ to } 0.68,\\
&1/H = (0.31522/s^{2.62435}) - 0.11714\, s^2 + 0.15756\, s - 0.05285\\
&\text{for } s \geqslant 0.68 \text{ to } 0.90,\\
&1/H = (0.31345/s^{2.64267}) - 0.09155\, s^2 + 0.14701\, s - 0.05877\\
&\text{and for } s \geqslant 0.90 \text{ to } 1.00,\\
&1/H = (0.30715/s^{2.84636}) - 0.69116\, s^3 + 1.08315\, s^2\\
&\qquad - 0.18341\, s - 0.20970
\end{aligned} \tag{3}$$

Equation (1) was obtained by applying the well-known Young-Laplace equation (4) to a pendant drop

$$\sigma(1/R_1 + 1/R_2) = \Delta P \tag{4}$$

where ΔP is the difference in pressure across the interface, and R_1 and R_2 are radii of curvatures at the interface. A working equation (1) was derived from a second-order differential equation of Andreas and Tucker [4] on the profile of the pendant drop, introducing the parameters d_e and d_s into Eq. (4). Fordham [5], Mills [6], and Staufer [7] numerically solved the differential equation to a sufficient degree of accuracy, and a table of

s vs $1/H$ was constructed. Based on this table, Misak prepared Eq. (3) describing $1/H$ in terms of s, which represents the values of s vs $1/H$ very accurately. In the present study, two diameters, d_e and d_s, were measured from the profile photograph of a pendant drop, and then the surface and the interfacial tensions were calculated by Eqs. (1) and (3). This method is a static one and is suitable for measurements at elevated pressures and temperatures. The notable merit of this method is that it is free from the effect of the contact angle between the sample liquid and the capillary tube at the end of which the pendant drop is formed.

3. EXPERIMENTAL APPARATUS, PROCEDURES, AND SAMPLES

3.1. Apparatus and Procedures

A schematic diagram of the experimental apparatus is shown in Fig. 2. The apparatus consists of mainly four parts: the pendant drop cell (1), the fluid supply units (2, 3), the temperature measurement system (4–6), and the pressure measurement system (7, 8, 11). In the pendant drop cell (1) at the desired temperature and saturation pressure, the pendant drop of the sample liquid is formed. The fluid supply units (2, 3) in Fig. 2 are made of stainless steel. The sample liquid is introduced into the cell by a plunger of a supply unit, and the pendant drop of the sample liquid is formed. The size of the drop can be controlled. The temperature measurement system (4–6) consists of a C–C sheathed thermocouple, a digital multimeter, and a cold junction. The thermocouple is placed in the cell (1), and the distance between the tip of the thermocouple and the pendant drop is about 3 mm. The pressure measurement system (7, 8, 11) consists of Bourdon gauges

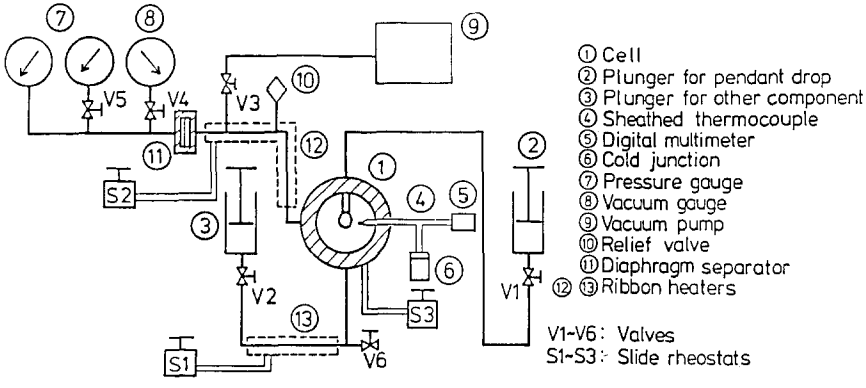

Fig. 2. Pendant drop apparatus.

and a diaphragm separator (11), which prevents the contamination of pressure transmitting fluid into the measurement system. The temperature in the separator and the connecting tubes is controlled by ribbon heaters (12) and maintained at a temperature slightly higher than that in the cell in order to prevent the condensation of the saturated vapor onto the inner walls of the tubes and the separator. A cross section of the pendant drop cell (1) is shown in Fig. 3. The Pyrex glass windows (2) and stainless-steel cylinders (3) are on both sides of the stainless-steel cell. An aluminum cylinder (4) is used to get a uniform temperature field. The temperature was controlled by heaters (7). The capillary tubes, at the end of which the pendant drop of the sample liquid is formed, are made of Pyrex glass (o.d., 3.0 mm) or stainless steel (o.d., 1.0 mm). The diameters d_e and d_s of the drop were measured using the precalibrated diameter of the capillary tube as the reference. Figure 4 shows the optical system, which consists of a microscope illuminator, a light diffuser, a heat filter filled with water, and a 35-mm camera with a 100-mm f4 macrographic lens and bellows. These components, together with the pendant drop cell, are aligned and fixed on a massive iron optical bench, which is mounted on a vibration isolator equipped with pressurized air supports regulated by an automatic level controller. After the cell, the tube, and the diaphragm separator were heated to the desired temperature, the sample liquids or vapors were led into the cell. Having confirmed that the pressure and the temperature were in an equilibrium state for about an hour, a pendant drop of a sample

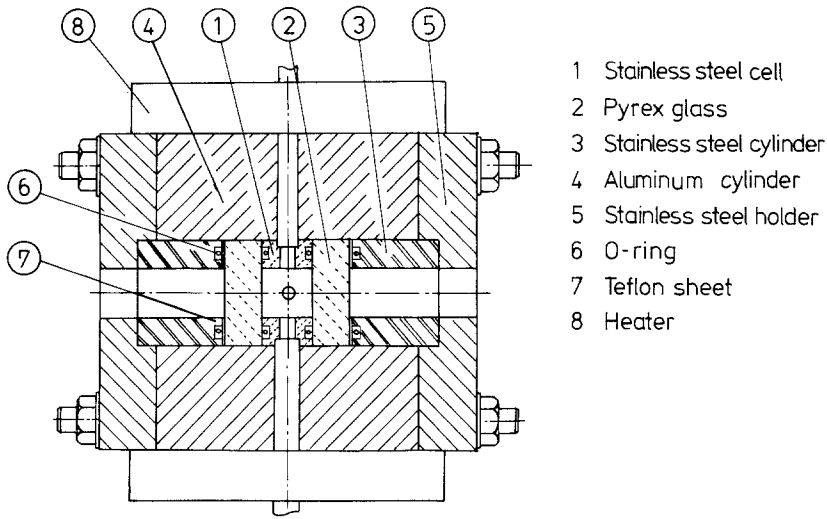

Fig. 3. Construction of the pendant drop cell.

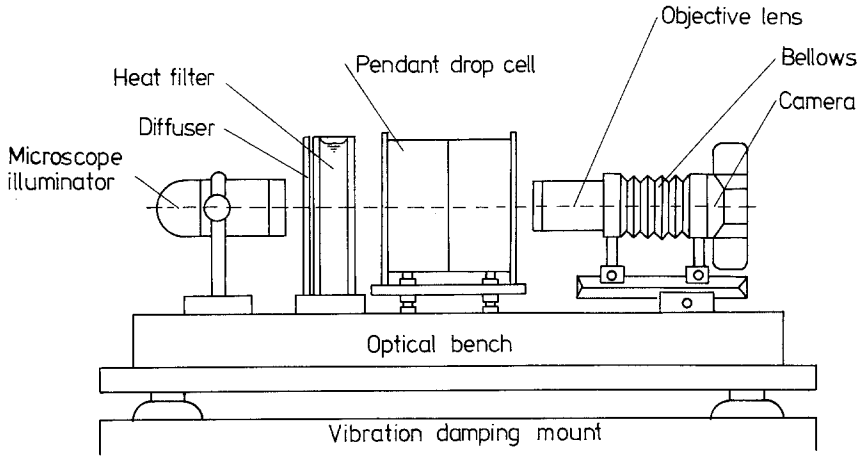

Fig. 4. Optical system (not to scale).

liquid was formed on the tip of the capillary tube and held still for at least 10 min. Then seven or eight pictures of each pendant drop were taken, varying the size of the drop of check the reproducibility under constant temperature and pressure. On the negative photo film, diameters d_e and d_s and the diameter of the capillary tube were measured by a film analyzing system, which consists of a film projector and a screen box with builtin X–Y traveling cross hairs linked to a digital readout device. The diameter of the capillary tube was measured before assembly and corrected for thermal expansion of the material.

3.2. Samples

Water was distilled once and then treated with a reverse-osmosis device and an ion exchanger. The densities of the water and vapor were calculated with the aid of the IFC Formulation for Industrial Use (1967) [8]. The *n*-pentane (C_5H_{12}) was of reagent grade and the purity was better than 99 wt%. The density of *n*-pentane was calculated by the following equation, which was recently correlated based on the data in Ref. 9:

$$\rho = A(0) + A(1)T + A(2)T^2 + A(3)T^3 \tag{5}$$

where

$$A(0) = 6.517 \times 10^{-1}$$

$$A(1) = -1.265 \times 10^{-3}$$

$$A(2) = 3.273 \times 10^{-6}$$

$$A(3) = -2.275 \times 10^{-8}$$

ρ is the density of *n*-pentane in $kg \cdot m^{-3}$ and T is the temperature in °C. The uncertainty of the density of liquid *n*-pentane in Ref. 9 was $\pm 0.5\%$. The density of saturated vapor of *n*-pentane was calculated by a virial equation of state. The second virial coefficient was taken from API Research Project 44 [10]. R 113 ($C_2Cl_3F_3$) was of reagent grade and the purity was 99.991 wt% or better. The densities of saturated liquid and vapor of R 113 were calculated by the equation of Mastroianni [11]. The uncertainty of the density was estimated as $\pm 0.1\%$.

4. RESULTS

Reliability of the apparatus was checked by measuring beforehand the surface tension of water in the temperature range from 25.3 to 197.3°C at intervals of about 25°C. The reproducibility of this measurement was $\pm 0.5\%$. Figure 5 shows the deviations of the measured surface tension of water in this study from the recommended value of the IAPS [12]. The agreement is better than $\pm 0.5\%$. The uncertainty of the IAPS recommendation is from ± 0.22 to $\pm 0.36\ mN \cdot m^{-1}$ in the temperature range 25–200°C.

4.1. *n*-Pentane–Water System

The surface tension of water in contact with saturated vapors of water and *n*-pentane, σ_W, the interfacial tension between liquid *n*-pentane and

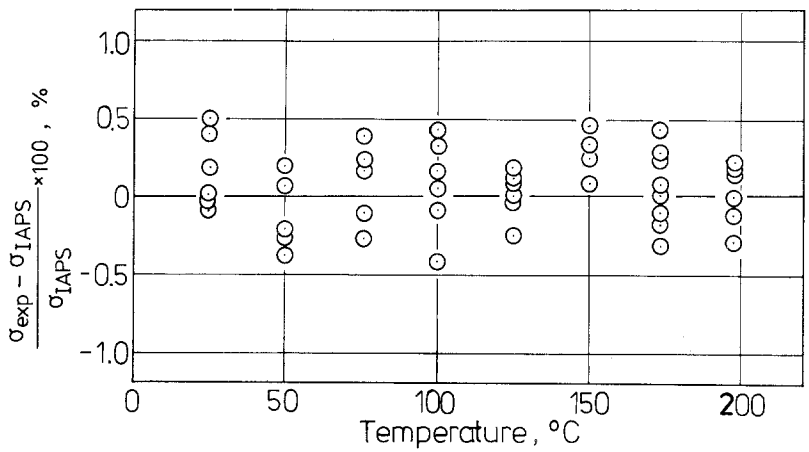

Fig. 5. Deviation of the measured surface tension of water from the recommended value of the IAPS.

Table I. The Surface and Interfacial Tensions in the *n*-Pentane–Water System

Measured surface tension of *n*-pentane saturated with water vapor system		Measured interfacial tension of *n*-pentane–water system		Measured surface tension of water saturated with *n*-pentane vapor system	
T (°C)	σ (mN · m^{-1})	T (°C)	σ (mN · m^{-1})	T (°C)	σ (mN · m^{-1})
20.2	16.19	26.3	48.71	23.3	62.13
52.8	12.70	51.8	46.67	49.5	58.26
76.5	10.36	82.7	44.23	75.1	52.57
101.0	7.83	106.6	41.03	101.8	47.00
123.7	5.57	129.0	37.87	124.9	39.27
148.9	3.20	149.6	33.88	149.1	33.21

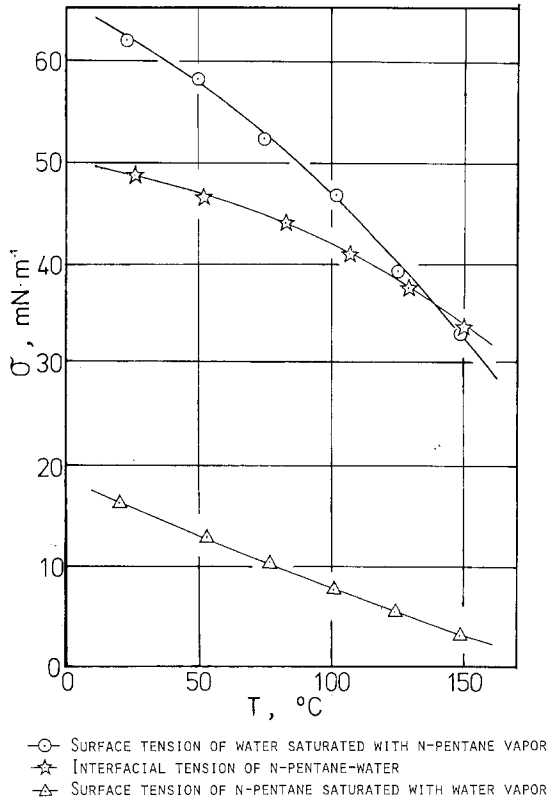

Fig. 6. Temperature dependences of the measured surface and interfacial tensions in the *n*-pentane–water system.

liquid water, $\sigma_{W\cdot P}$, and the surface tension of *n*-pentane contacting with saturated vapor of water and *n*-pentane vapor, σ_P, were measured from room temperature to about 150°C at intervals of 25°C. Measurements were repeated five to eight times at each temperature. The averaged values are shown in Table I. Reproducibilities of measured values of σ_W, $\sigma_{W\cdot P}$, and σ_P are ± 1.0, ± 0.7, and $\pm 1.4\%$, respectively. Figure 6 shows the temperature dependences of the measured surface and the interfacial tensions.

4.2. R 113–Water System

The surface tension of water in contact with saturated vapors of water and R 113, σ_W, the interfacial tension between liquid R 113 and water, $\sigma_{R\,113\cdot W}$, and the surface tension of R 113 in contact with saturated vapors of water and R 113, $\sigma_{R\,113}$, were measured from room temperature to about 150°C at intervals of 25°C. Data given in Table II are averages of five to eight repeated measurements at each temperature. Reproducibilities of measured values of σ_W, $\sigma_{R\,113\cdot W}$, and $\sigma_{R\,113}$ are ± 0.7, ± 1.5, and $\pm 1.1\%$, respectively. Figure 7 shows the temperature dependences of these surface and interfacial tensions.

4.3. Error Analysis

The errors of the surface and the interfacial tensions were calculated considering errors in d_e and d_s, the densities of liquids and vapors, the thermal expansion, and gravity constants. The error in the thermal expansion coefficient of Pyrex glass or SUS 304 was estimated to be a few

Table II. The Surface and Interfacial Tensions in the R 113–Water System

Measured surface tension of R 113 saturated with water vapor system		Measured interfacial tension of R 113–water system		Measured surface tension of water saturated with R 113 vapor system	
T (°C)	σ (mN·m^{-1})	T (°C)	σ (mN·m^{-1})	T (°C)	σ (mN·m^{-1})
20.0	17.71	21.5	44.18	26.6	58.26
51.8	14.18	51.1	42.15	51.2	55.66
76.6	11.79	69.3	40.73	75.7	52.16
97.3	9.62	98.4	37.32	100.2	48.47
123.0	7.12	125.6	34.34	124.6	43.26
151.8	4.44	148.0	30.97	150.2	37.91

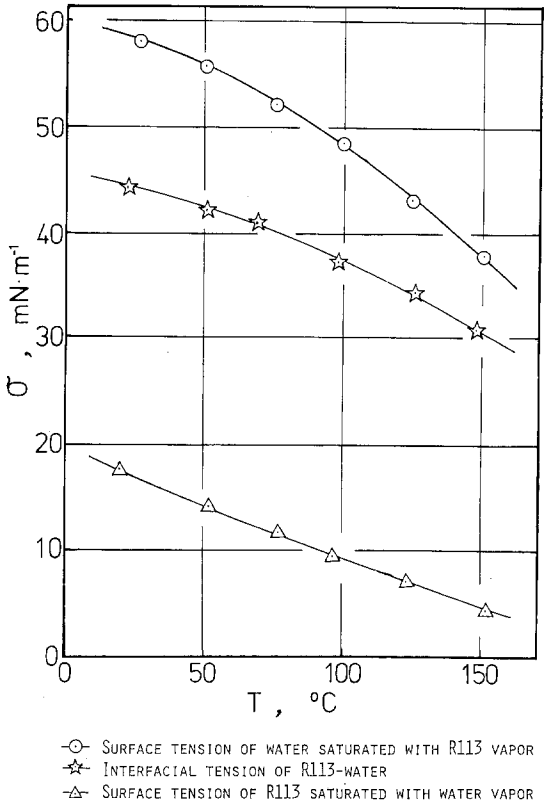

Fig. 7. Temperature dependences of the measured surface and the interfacial tensions in the R 113–water system.

percent [13]. The errors in the surface or the interfacial tensions due to errors in the thermal expansion coefficient and the gravity constant were negligible. For the surface tension of water, the maximum error was estimated to be $\pm 0.9\%$, due mainly to errors in d_e and d_s and the error in the density of *n*-pentane were estimated to be ± 0.5 and $\pm 0.9\%$, respectively. Therefore, the maximum error in the interfacial tension between liquid *n*-pentane and liquid water was estimated to be $\pm 1.4\%$. Similarly, the maximum errors in σ_W and σ_P were estimated to be ± 0.8 and $\pm 2.1\%$, respectively. For the R 113–water system, the maximum errors in the measurements of $\sigma_{R\,113\text{-}W}$, σ_W, and $\sigma_{R\,113}$ were estimated to be ± 1.5, ± 0.7, and $\pm 2.2\%$, respectively.

4.4. Correlations

Measured data of the surface and the interfacial tensions were correlated as a function of temperature. For the *n*-pentane–water system,

$$\sigma_W = 65.42 - 1.181 \times 10^{-1}\, T - 6.79 \times 10^{-4}\, T^2 \quad (6)$$

$$\sigma_{W\cdot P} = 49.32 - 1.417 \times 10^{-2}\, T - 5.89 \times 10^{-4}\, T^2 \quad (7)$$

$$\sigma_P = 18.38 - 1.095 \times 10^{-1}\, T + 5.06 \times 10^{-5}\, T^2 \quad (8)$$

and for the R 113–water system,

$$\sigma_W = 60.39 - 6.387 \times 10^{-2}\, T - 5.75 \times 10^{-4}\, T^2 \quad (9)$$

$$\sigma_{R\,113\cdot W} = 45.31 - 4.372 \times 10^{-2}\, T - 3.58 \times 10^{-4}\, T^2 \quad (10)$$

$$\sigma_{R\,113} = 19.90 - 1.128 \times 10^{-1}\, T + 7.20 \times 10^{-5}\, T^2 \quad (11)$$

Equations (6)–(8) represent the measured data for the *n*-pentane–water system with a mean deviation of ± 0.4–$\pm 1.2\%$, depending on the temperature range. Equations (9)–(11) represent the measured data for the R 113–water system with a mean deviation of ± 0.5–$\pm 0.7\%$.

5. DISCUSSION

5.1. Surface and Interfacial Tensions

Figure 8 shows a comparison of the previously reported interfacial tension between water and *n*-pentane with those of the present study. The value of Aveyard and Haydon [14] by the drop weight method is higher by 3% than that of the present study. The values of Donahue and Bartell [15] by the pendant drop method agree with those of the present study within the experimental uncertainty. The values of Mori et al. [16] by the pendant drop method show a reasonable agreement and the deviation is about 1%, which is within the experimental uncertainty of both studies. For σ_W and σ_P, only Mori et al. [16] reported data which fall within about 1% from those in this study. For the R 113–water system, Ref. 16 is the only reference to be compared with the present study. It suggests that the uncertainty of the interfacial tension in Ref. 16 might be larger than the 1.3% quoted by the authors because of the difficulty in forming a pendant drop. For $\sigma_{R\,113\cdot W}$, the values reported in Ref. 16 are higher than those of the present study by 1.5–1.8%. The σ_W values reported in Ref. 16 agree with the data of the present study.

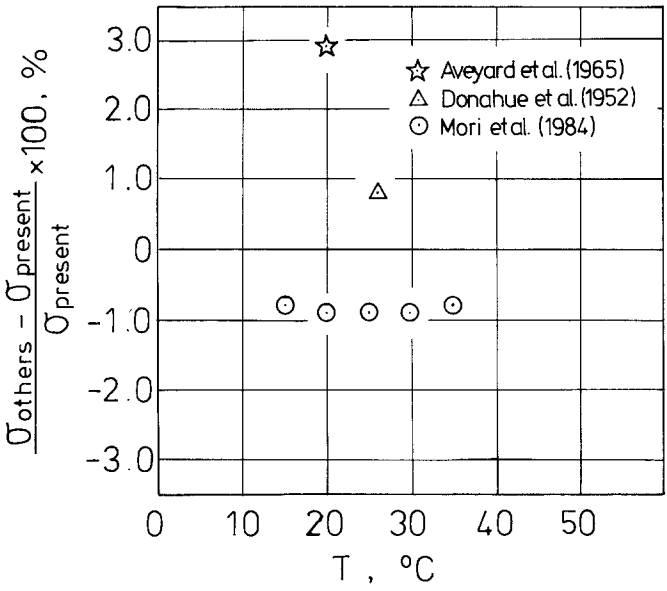

Fig. 8. Deviation of the previously reported interfacial tension between water and *n*-pentane from the present results.

5.2. Spreading Coefficients

The temperature dependence of the spreading coefficients in the *n*-pentane–water system was calculated from the measured surface and the interfacial tensions as represented by Eqs. (12)–(14) and shown in Fig. 9.

$$S_{P/W} = -2.27 + 7.55 \times 10^{-3}\, T - 1.41 \times 10^{-4}\, T^2 \tag{12}$$

$$S_{W/P} = -96.36 + 2.470 \times 10^{-2}\, T + 1.319 \times 10^{-3}\, T^2 \tag{13}$$

$$S_{Vapor/PW} = -34.48 + 2.115 \times 10^{-1}\, T + 3.97 \times 10^{-5}\, T^2 \tag{14}$$

The positive value of the spreading coefficient $S_{1/2}$ means that liquid 1 spreads on liquid 2, which is immiscible with liquid 1. If negative, liquid 1 does not spread and forms a configuration of a lens on liquid 2. The spreading coefficient is also necessary to predict the shape of the two-phase bubble, which is formed in, for example, the process of direct-contact heat transfer with evaporating drops in a hotter medium or condensing bubbles in a colder medium. For these systems we suppose that two liquids are immisible. Adamson [17] reported the spreading coefficient of *n*-pentane on water, $S_{P/W}$, as $-0.22\ \mathrm{mN \cdot m^{-1}}$ at 15°C. $S_{P/W}$ and $S_{W/P}$ are also reported in the Ref. 16. In Fig. 9, these two previous results are compared with

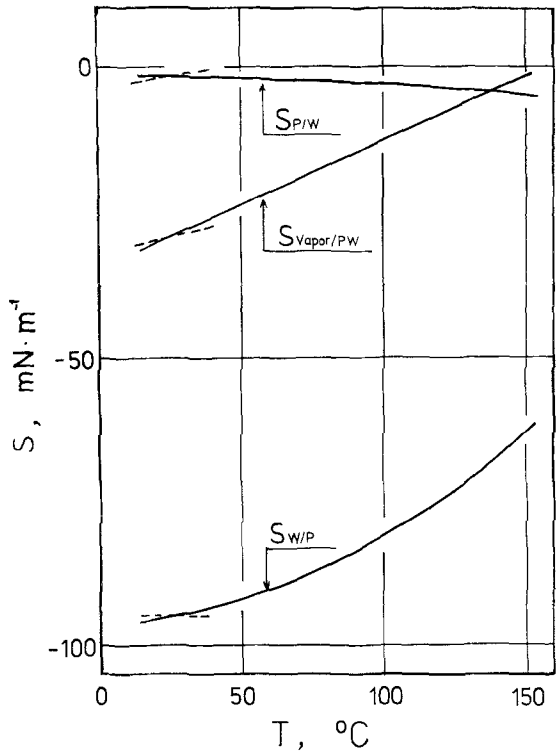

Fig. 9. Temperature dependences of the spreading coefficients in the *n*-pentane–water system.

those of the present study. Although the spreading coefficients agree with each other in the temperature range from 20 to 30°C, the temperature dependences over a temperature range in each study show some difference. But the temperature ranges covered in previous investigations are not wide enough to permit a more thorough study. As shown in Fig. 9, $S_{P/W}$ of the present study shows a negative temperature dependence, while the temperature dependence in Ref. 16 is positive. For the R 113–water system, the spreading coefficients are calculated from the measured surface and interfacial tensions and are represented by Eqs. (15)–(17) and are shown in Fig. 10.

$$S_{R\,113/W} = -4.83 + 9.26 \times 10^{-2}\, T - 2.89 \times 10^{-4}\, T^2 \qquad (15)$$

$$S_{W/R\,113} = -85.80 - 5.2 \times 10^{-3}\, T + 1.004 \times 10^{-3}\, T^2 \qquad (16)$$

$$S_{Vapor/R\,113\,W} = -34.98 + 1.329 \times 10^{-1}\, T + 1.45 \times 1^{-4}\, T^2 \qquad (17)$$

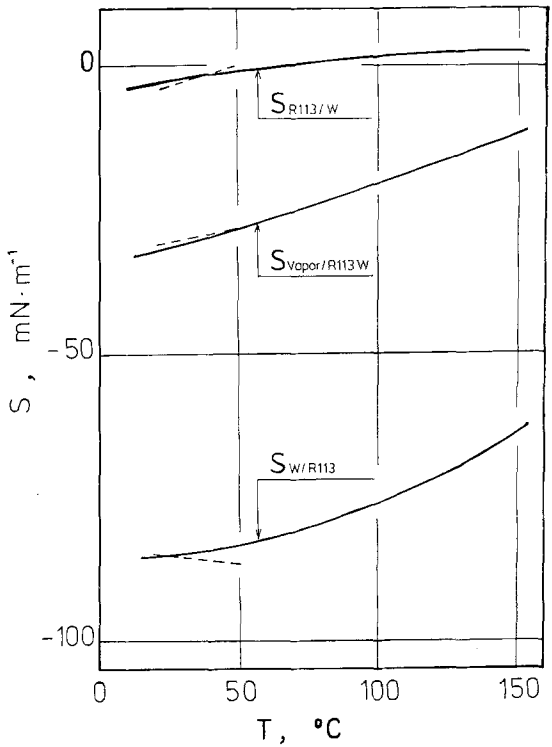

Fig. 10. Temperature dependences of the spreading coefficients in the R 113–water system.

The temperature dependences of $S_{W/R\,113}$ and $S_{Vapor/R\,113\,W}$ are positive. And the value of $S_{R\,113/W}$ changes its sign from negative to positive at about 70°C. The temperature dependences of $S_{R\,113/W}$ and $S_{vapor/R\,113\,W}$ in Ref. 16 are quite similar to those in this study, while that of $S_{W/R\,113}$ in Ref. 16 appears to be different and negative.

5.3. Film Pressure

The temperature dependences of the film pressure in the *n*-pentane–water system and R 113–water system were calculated and represented by Eqs. (18) and (19) and are shown in Fig. 11.

$$\Pi_{P\text{-}W} = 10.34 - 2.69 \times 10^{-2}\, T + 4.44 \times 10^{-4}\, T^2 \tag{18}$$

$$\Pi_{R\,113\text{-}W} = 15.39 - 8.156 \times 10^{-2}\, T + 3.417 \times 10^{-4}\, T^2 \tag{19}$$

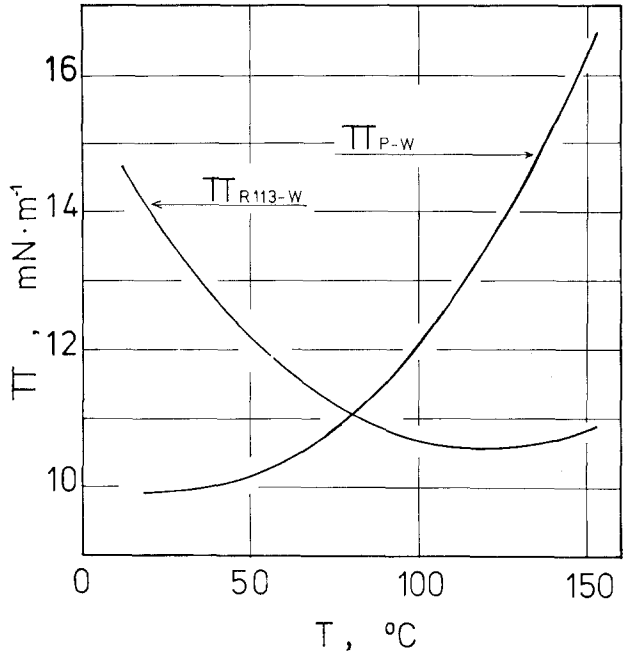

Fig. 11. Temperature dependences of the film pressure in the *n*-pentane–water system and R 113–water system.

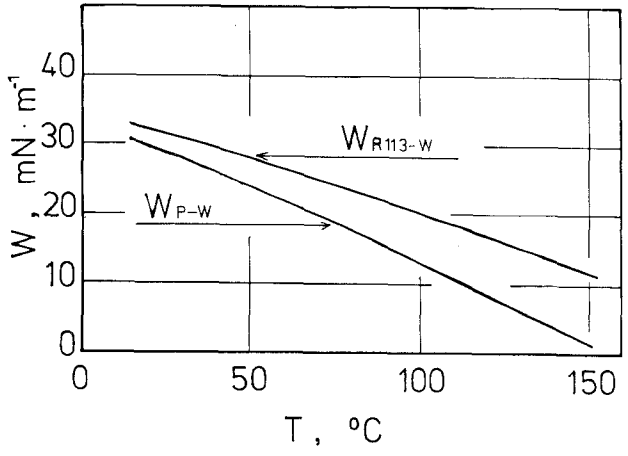

Fig. 12. Temperature dependences of the work of adhesion in the *n*-pentane–water system and R 113–water system.

For the *n*-pentane–water system, the film pressure increases with increasing temperature, which indicates that the effect of *n*-pentane vapor on the surface of water increases with increasing temperature. For the R 113–water system, the film pressure first decreases with increasing temperature and begins to increase at 130°C.

5.4. The Work of Adhesion

The work of adhesion, defined as $W_{12} = \sigma_1 + \sigma_2 - \sigma_{12}$, was calculated for the *n*-pentane–water and R 113–water systems, and is shown in Fig. 12. In each system, the work of adhesion shows a negative temperature dependence.

ACKNOWLEDGMENTS

The authors thank Mr. H. Tsujino for help in the measurements and Mr. Y. Uota for his help in the preparation of the manuscript.

REFERENCES

1. K. Higeta, Y. H. Mori, and K. Komotori, *AIChE Symp. Ser.* **75**(189):256 (1979).
2. Y. H. Mori, K. Nagai, and K. Komotori, *Trans. ASME J. Heat Transfer* **103**(3):508 (1981).
3. M. D. Misak, *J. Colloid Interface Sci.* **27**(1):141 (1968).
4. J. M. Andreas and W. B. Tucker, *J. Phys. Chem.* **42**:1001 (1938).
5. S. Fordham, *Proc. Roy. Sci.* **194A**:1 (1948).
6. O. S. Mills, *Br. J. Appl. Phys.* **4**:247 (1953).
7. C. E. Staufer, *J. Phys. Chem.* **69**(6):1933 (1965).
8. *1980 SI JSME Steam Tables*, 4th ed. (Japan Society of Mechanical Engineers, Tokyo, 1981), p. 106.
9. V. M. Berry and B. H. Sage, *Phase Behavior in Binary and Multicomponent Systems at Elevated Pressures: n-Pentane and Methane-n-Pentane*, Natl. Stand. Ref. Data Ser., NBS 32 (NBS, 1970).
10. API Research Project 44, 2, Table 23-2-(1,101)-h (1970).
11. M. J. Mastroianni, *J. Chem. Eng. Data* **23**(2):113 (1978).
12. *1980 SI JSME Steam Tables*, 4th ed. (Japan Society of Mechanical Engineers, Tokyo, 1981), p. 105.
13. Y. S. Touloukian, P. E. Liley, and S. C. Saxena, *Thermophysical Properties of Matter, Vol. 12 Thermal Expansion—Metallic Elements and Alloys* (Plenum, New York, 1970).
14. R. Aveyard and D. A. Haydon, *Trans. Faraday Soc.* **61**(10):2255 (1965).
15. D. J. Donahue and F. E. Bartell, *J. Phys. Chem.* **56**(4):480 (1952).
16. Y. H. Mori, N. Tsui, and M. Kiyomiya, *J. Chem. Eng. Data* **29**(4):407 (1984).
17. A. W. Adamson, *J. Colloid Interface Sci.* **27**:2 (1968).